SEMARAK ILMU PUBLISHING

Semarak International Journal of Electronic System Engineering

Journal homepage:
https://semarakilmu.my/index.php/sijese/index
ISSN: 3030-5519

Thermal and Electrical Properties of Zinc-Strontium-Lithium Phosphate Glass Doped with Carboxymethyl Cellulose

Siti Norfariza Farhana Mohd Razak[1], Farhana Mohamiddin[1], Nurhafizah Hasim[1,*], Nur Hidayah Ahmad[1], Norshahirah Mohamad Saidi[1], Mohd Fuad Mohamad[2], Anis Nazihah Mat Daud[3]

[1] Advanced Optical Materials Research Group, Faculty of Science, Universiti Teknologi Malaysia, Johor, Skudai, 81310, Malaysia
[2] Department of Chemistry, Faculty of Science, Universiti Teknologi Malaysia, Johor, Skudai, 81310, Malaysia
[3] Department of Physics, Faculty of Science and Mathematics, Universiti Pendidikan Sultan Idris, 35900 Tanjung Malim, Perak, Malaysia

ARTICLE INFO

Article history:
Received 23 October 2025
Received in revised form 30 October 2025
Accepted 20 November 2025
Available online 27 November 2025

Keywords:
Phosphate glass; DTA; EIS

ABSTRACT

The influence of Carboxymethyl Cellulose (CMC) on the thermal and electrical properties of phosphate glass has attracted considerable attention, yet its mechanistic role in modifying glass structure remains insufficiently understood. This study aims to synthesize and characterize phosphate glasses with composition $(40-x)P_2O_5–30ZnO–25Li_2O–5SrO–(x)CH_2COOH$ ($0.0 \leq x \leq 0.5$ mol%) to elucidate how CMC incorporation reshapes the glass network and alters its physical, thermal, and electrical behavior. The glasses were prepared by melt-quenching and characterized using XRD, DTA, and EIS analyses. Density increased from 2.604 to 3.194 g/cm³ and molar volume decreased to 29.326 $cm^3 \cdot mol^{-1}$ at 0.2 mol% CMC, indicating stronger network compaction. The optimal composition at 0.2 mol% CMC exhibited the highest ionic conductivity (2.89×10^{-7} $S \cdot cm^{-1}$) and lowest activation energy (1.20×10^{-2} eV). This enhancement arises from CMC's carboxylate groups, which form hydrogen-bonded linkages with phosphate tetrahedra and stabilize Li^+ pathways within the matrix. The findings demonstrate that low-level CMC addition effectively tunes network rigidity, ionic mobility, and dielectric response, providing a green and sustainable strategy for tailoring the performance of phosphate-based functional glasses.

1. Introduction

Glass is a promising material for making small-scale components and devices because it offers a unique set of properties useful for many applications. These include strong mechanical and thermal performance, clear optical transparency, chemical resistance, and the ability to be reused or recycled. Glass materials exhibit high breakdown strength but a relatively low dielectric constant (ε_r). Several efforts have been made to enhance ε_r while maintaining strong breakdown performance. However, molten phosphate glasses are highly corrosive to refractory linings, which has restricted their practical applications [1]. A modifier is widely used to adjust and enhance the physical and chemical

* *Corresponding author.*
E-mail address: nurhafizah.h@utm.my

https://doi.org/10.37934/sijese.7.1.2232

properties of the glass network and it is a compound added to alter the behavior or characteristics of the material. ZnO is considered an excellent substitute for developing stable glasses with a low transformation temperature (T_f) [2]. The glass transition temperature (T_g) varies depending on the glass composition. The incorporation of ZnO appears to reduce the condensation of metaphosphate chains, as evidenced by the increase in T_g value, indicating a modified glass network. Moreover, ZnO has attracted significant attention due to its distinctive properties, including a wide band gap (~3.37 eV) and high dielectric constant, which enable its application in optical and electronic devices such as light-emitting diodes (LEDs) and laser diodes [3].

Strontium oxide (SrO) is known for its important role in bone repair, and since phosphate glasses have a structure similar to the mineral part of bones, studying the effect of SrO on their structural and physical properties is valuable. However, phosphate glasses generally have poor chemical durability because their P–O–P bonds can easily react with water, making them susceptible to corrosion in humid environments. The issue can be effectively overcome by incorporating alkaline earth oxides, such as strontium oxide (SrO), which significantly improve the chemical stability and durability of glass materials. The addition of SrO to pure phosphate glass helps form a metaphosphate structure, which strengthens the glass network and improves its overall stability [9]. The incorporation of Li_2O in P_2O_5-based glasses has been shown to play a significant role in improving ionic conductivity, as Li^+ ions possess a smaller ionic radius (0.76 Å). This smaller size allows for easier ion mobility within the glass matrix, resulting in enhanced electrical performance. Furthermore, the addition of Li_2O leads to the breakdown of P–O–P bridging bonds, generating non-bridging oxygen (NBO) atoms that modify the glass network structure. Moreover, the addition of Li_2O as a glass network modifier helps generate intermediate energy transfer bands, facilitating the transfer of energy from the host matrix to the RE ions and thereby enhancing the luminescence intensity of the glass [4]. Stable phosphate glasses are often developed by combining P_2O_5 with transition metal oxides such as ZnO and alkali metal oxides like Li_2O [5].

In phosphate glass research, carboxymethyl cellulose (CMC) plays an important role, particularly in the fabrication of composite scaffolds for bone regeneration. Carboxymethyl cellulose (CMC) is an anionic, water-soluble derivative of cellulose, a linear polysaccharide made up of anhydro-glucose units. CMC films are well known for their excellent barrier properties against lipids, carbon dioxide, and oxygen. Because CMC is odorless, tasteless, non-caloric, and physiologically inert, it is widely used in food products and packaging as a thickener, emulsion stabilizer, adhesive agent, and moisture binder [6]. The replacement of some hydroxyl groups in cellulose with carboxymethyl groups enhances its water solubility and biocompatibility, making CMC suitable for a wide range of industrial and biomedical applications. While phosphate glasses have been widely studied for their thermal stability and electrical behavior, the specific influence of Carboxymethyl Cellulose (CMC) incorporation on their thermal and electrical properties remains insufficiently explored. Limited research has addressed how CMC interacts within the zinc–strontium–lithium phosphate glass network and its potential to enhance glass performance, indicating a need for further investigation in this area.

This study presents a hybrid organic–inorganic modification route, where CMC functions simultaneously as a structural modifier and conductivity enhancer. CMC's carboxylate ($–COO^-$) and hydroxyl (–OH) groups can coordinate with Li^+, Zn^{2+}, and Sr^{2+} cations, thereby influencing glass compactness and ionic transport behavior [14]. Unlike typical oxide additives, CMC introduces local hydrogen-bonded domains that can alter both rigidity and segmental motion. The present work provides new insight into how small fractions of CMC (0.0–0.5 mol%) can balance network consolidation and mobility, achieving an optimum conductivity and thermal stability near 0.2 mol%—a composition window never previously reported for phosphate glass systems.

Although phosphate glasses containing oxides such as ZnO, Li_2O, and SrO have been widely investigated for their electrical and thermal stability, the impact of organic biopolymer dopants on glass structure remains poorly understood. In particular, carboxylate-bearing macromolecules like Carboxymethyl Cellulose (CMC) offer dual functionality: introducing organic linkers capable of forming hydrogen bonds while altering network connectivity through the generation of non-bridging oxygens (NBOs) as mentioned in [15]. Despite the growing interest in hybrid and eco-friendly materials, no comprehensive study has clarified how CMC modifies phosphate network packing density, free volume, or ion transport pathways. Previous works have mainly reported inorganic dopants such as CuO, Er_2O_3, and rare-earths, but the structure–property correlation for organic dopants in phosphate glass systems is yet to be elucidated. This study aims to prepare and characterize (40 – x) P_2O_5 + 30ZnO + 25Li_2O + 5SrO + (x) CH_2COOH glass system using the melt-quenching method, focusing on evaluating its physical, thermal, and electrical properties.

2. Methodology

2.1 Experimental Method

Glass samples with the composition (40 − x)P_2O_5–30ZnO–25Li_2O–5SrO–(x)CH_2COOH (0.0 ≤ x ≤ 0.5 mol%) were synthesized via the melt-quenching method, where P_2O_5 acted as the network former, ZnO, Li_2O, and SrO as modifiers, and CH_2COOH as the dopant. Six samples (S1–S6) were prepared according to the molar ratios listed in Table 1. Each 10 g batch was accurately weighed, mixed for 30 minutes using a Labmill-800 milling machine, and preheated at 300 °C for 1 hour to remove moisture. The mixture was then melted at 1000 °C for 30 minutes in an alumina crucible and poured onto a stainless-steel plate preheated to 300 °C. The resulting glass was annealed at 300 °C for 3 hours to relieve internal stress and slowly cooled to room temperature overnight. Finally, the glass samples were polished using sandpaper to obtain smooth, uniform surfaces. The overall preparation process is shown in Fig. 1.

Table 1 The composition of (40 - x) P_2O_5 - 30ZnO - 25Li_2O- 5SrO – (x) CH_2COOH glass system.

Sample	Mol percentage of sample (%)				
	P_2O_5	ZnO	Li_2O	SrO	CH_2COOH
S1	40.0	30.0	25.0	5.0	0.0
S2	39.9	30.0	25.0	5.0	0.1
S3	39.8	30.0	25.0	5.0	0.2
S4	39.7	30.0	25.0	5.0	0.3
S5	39.6	30.0	25.0	5.0	0.4
S6	39.5	30.0	25.0	5.0	0.5

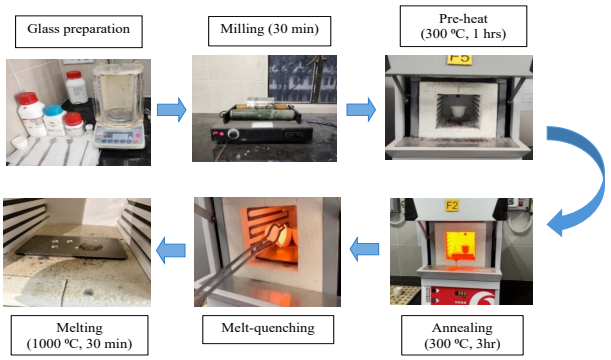

Fig. 1. Procedure of glass preparation

2.1.1 Density Analysis

The density of the six glass samples was measured using a Mettler Toledo density meter based on Archimedes' principle. Each sample was weighed in air and then in distilled water, with the setup calibrated beforehand. Measurements were repeated three times for accuracy, and the average values were used to calculate density. The molar volume of each glass sample was then determined using Eqs. (1)–(4).

$$\rho_{glass} = \frac{M_{air}}{M_{air} - M_{liquid}} \times \rho_{liquid} \quad (1)$$

The density of the glass samples (ρ_{glass}) was measured using the Archimedes' principle. In this method, ρ_{liquid} represents the density of the water used (0.99 g·cm^{-3}), while M_{air} and M_{liquid} refer to the weights of the sample measured in air and in water, respectively.

$$V_m = \frac{M}{\rho} \quad (2)$$

The density of the glass samples was determined using the Archimedes method. Based on the measured density (ρ) and the molecular weight (M) of the glass, calculated from the batch composition, the molar volume (V_m) was then determined using the following equation.

$$V_t = \Sigma \frac{V_i X_i}{V_m} \quad (3)$$

However, certain fundamental structural parameters, such as packing density (V_t), play an important role. The atomic packing density (V_t) is defined as the ratio of the effective volume of the glass to the minimum theoretical volume occupied by the ions, as expressed by the following equation. V_i and X_i represent the packing factor and mole fraction of the oxides, respectively, while the total number of oxygen atoms and the fraction of oxygen atoms are also considered in the calculation.

$$V_i = 6.032 \times 10^{23} \times \frac{4}{3}\pi \left(X R_A^3 + Y R_O^3\right) \quad (4)$$

where R_A and R_O denote the ionic radii of the metal ion (A) and oxygen (O), respectively.

2.1.2 X-Ray Diffraction (XRD)

The glass samples were ground into fine powder and analyzed using a Rigaku SmartLab diffractometer with Cu Kα radiation (λ = 1.5405 Å) over a 2θ range of 5°–90° to determine their amorphous or crystalline nature.

2.1.3 Differential Thermal Analysis

Thermal behavior, including T_g, T_c, and T_m, was examined using a Shimadzu DTA analyzer with Al_2O_3 as reference. About 10–15 mg of powdered sample was heated from 0°C to 1000°C at 10°C/min under nitrogen flow.

2.1.4 Electrical Impedance Spectroscopy (EIS)

Polished samples were coated with silver paint to form electrodes and connected with copper wires. Measurements were taken at room temperature using a Hioki LCR meter across 50 Hz–1 MHz. Bulk resistance (Rb) was obtained from impedance plots (Z_i vs Z_r), and electrical conductivity and activation energy were calculated using Eqs. (5) and (6).

$$Z^*_{CPE} = \frac{1}{A_0(j\omega)^n} \quad (5)$$

where Z* is a complex impedance and j is an imaginary unit.

$$\sigma = \frac{t}{R_b A} \quad (6)$$

The bulk resistance (R_b) was determined from the plot of imaginary impedance (Z_i) against real impedance (Z_r), and the ionic conductivity (σ) was subsequently calculated based on the obtained R_b value and t represents the thickness of the sample, and A (cm^2) denotes its cross-sectional area.

3. Results & Discussion

3.1 Glass Sample Preparation

Glass samples with the composition $(40 - x)P_2O_5–30ZnO–25Li_2O–5SrO–(x)CH_2COOH$ ($0.0 \leq x \leq 0.5$ mol%) were synthesized via the melt-quenching method. All glasses were transparent and colorless, as shown in [7]. Each sample was then characterized for physical, thermal, and electrical properties to assess the effect of composition.

3.2 Physical Analysis

The density of the glass samples was determined using Eq. (1) to Eq. (4) based on Archimedes' principle. From the obtained density values, additional physical parameters such as molar volume and ionic packing density were also calculated. Fig. 2 shows the relationship between the concentration of Carboxymethyl Cellulose (CMC) and the glass density of the $P_2O_5–ZnO–Li_2O–SrO–CH_2COOH$ system. The results indicate an increase in density from 2.604 to 3.194 g/cm^3 with CMC doping up to 0.2 mol%, followed by a decrease to 2.800 g/cm^3.

The observed rise in density and packing density up to 0.2 mol% CMC suggests stronger compaction of the phosphate network. The carboxylate and hydroxyl groups from CMC can form electrostatic linkages as mentioned in [16] with Li^+, Zn^{2+}, and Sr^{2+} ions, effectively reducing inter-tetrahedral spacing and generating short P–O–M bridges. This compact arrangement explains the decreased molar volume and improved rigidity. Beyond 0.2 mol%, excess CMC introduces additional non-bridging oxygens and free volume pockets as partial volatilization occurs during melting, causing density and packing to decline. Hence, CMC acts as a bifunctional agent that strengthens the network at low content and loosens it at higher concentrations.

The increase in glass density with CMC addition also suggests a modification in the rigidity of the glass network, mainly attributed to the larger relative mass and ionic radius of the CMC ions compared to the phosphate ions in the glass matrix. The molar volume of the glass increases between 0.3 and 0.5 mol% CMC, likely due to more non-bridging oxygen in the network. As CMC content rises, glass density increases while molar volume decreases because of shorter bond lengths. Figure 2 shows that Vm decreases from 36.039 to 29.326 $cm^3 \cdot mol^{-1}$ at 0.2 mol% CMC, then rises to 33.368 $cm^3 \cdot mol^{-1}$ at 0.5 mol%. P–O–Zn bridges are more ionic than P–O–P bridges, making the network more compact. Higher density results from stronger interactions between glass-forming anions and modifying cations [8].

Fig. 3 shows ionic packing density versus CMC concentration. Packing density rises from 0.203 to 0.249 $g \cdot cm^{-3}$ at 0.2 mol% CMC, then falls to 0.218 $g \cdot cm^{-3}$ at 0.5 mol%. The decrease in packing density with higher CMC increases molar volume, indicating a less rigid network due to the formation of non-bridging oxygens (NBOs). This breaks bonds and increases free volume, showing an inverse relationship between density and molar volume [9]. Adding CMC also improves the overall physical performance of the glass samples.

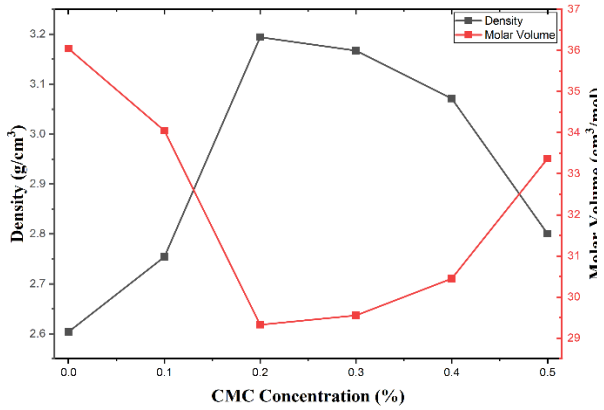

Fig.2. Density and molar volume against CMC concentration of glass (40 – *x*) P_2O_5 – 30ZnO – 25Li_2O – 5SrO – (*x*) CH_2COOH

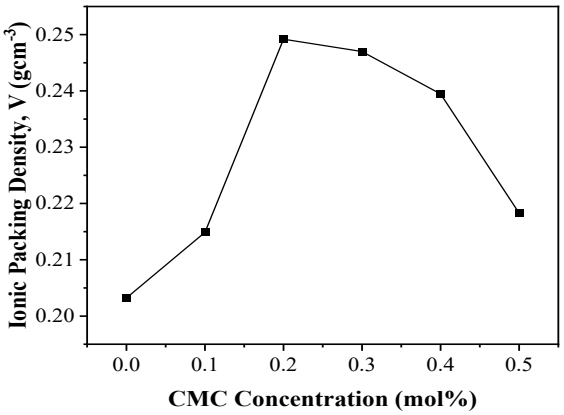

Fig.3. Ionic packing density against CMC concentration of glass (40 - *x*) P_2O_5 - 30ZnO - 25Li_2O - 5SrO – (*x*) CH_2COOH

3.3 X-Ray Diffraction (XRD) Analysis

Fig.4. shows the X-ray diffraction (XRD) spectrum of sample S6, which displays the broad diffuse bands characteristic of amorphous materials. The pattern exhibits only wide humps within the 10°–35° (2θ) range, with no sharp peaks, confirming the amorphous nature of the glass samples. The broad peaks at lower angles indicate the presence of long-range structural disorder within the glass matrix [10]. Additionally, the XRD data revealed that the amorphous halo shifts to lower angles with the substitution of SrO for ZnO. This shift is attributed to the larger ionic radius of Sr^{2+} compared to Zn^{2+}, suggesting an increase in the average interatomic spacing within the glass network.

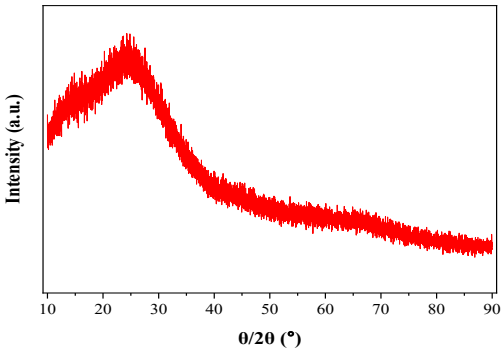

Fig.4. XRD pattern of P_2O_5—ZnO—Li_2O—SrO—CH_2COOH glasses of sample S6

3.4 Thermal Analysis

Figure 5 shows the DTA curves of the synthesized glasses with compositions (40 – x) P_2O_5–30ZnO–25Li_2O–5SrO–(x) CH_2COOH. Thermal stability was evaluated using key temperatures: glass transition (Tg), crystallization (Tc), melting (Tm), temperature difference (ΔT), and the Hruby parameter (H). In the DTA spectra, the first endothermic peak corresponds to Tg, the exothermic peak to Tc, and the final endothermic peak to Tm. Crystallization peaks for S1–S6 appeared at 489, 492, 495, 499, 503, and 489 °C, respectively, showing the development of a crystalline phase.

The increase in glass transition and crystallization temperatures up to 0.2–0.3 mol% reflects the enhanced connectivity produced by CMC–metal coordination. The formation of ionic bridges between carboxylate oxygens and divalent cations (Zn^{2+} and Sr^{2+}) reinforces the phosphate network, elevating thermal resistance. This indicates that the carboxylate and hydroxyl functional groups in CMC effectively interact with the modifier ions to strengthen the bonding energy within the glass matrix. Consequently, both Tg and Tc increase due to the formation of stronger P–O–Zn and P–O–Sr linkages.

However, the subsequent decrease in Tg at higher CMC loadings suggests that excessive organic content promotes micro-void formation and increases the number of non-bridging oxygens (NBOs), which leads to partial depolymerization of the network. This behavior is consistent with the structural relaxation observed in phosphate-based glasses containing organic modifiers. The Hruby parameter (H) trend further supports this dual mechanism, showing that an optimum rigidity which is mobility balance is achieved when CMC establishes a semi-crosslinked network without excessive disruption.

Table 2 shows that the Hruby criterion (H) increased from 0.770 to 1.222, while ΔT increased from 57 °C to 77 °C, indicating that the glasses exhibit high strength and good glass-forming ability [11]. Additionally, an increase in Tm was observed with increasing CMC content. The ΔT parameter was used to assess thermal stability, with higher values indicating better glass-forming ability and thermal resistance [20]. A larger ΔT and smaller Tm – Tc value corresponds to slower crystallization relative to devitrification, thus promoting glass formation. Among the studied compositions, S6 demonstrates the highest thermal stability, as reflected by its ΔT and Hruby criterion. The incorporation of CMC, together with the divalent modifier ions SrO and ZnO, creates ionic bridges between non-bridging oxygens, linking phosphate anions through electrostatic interactions. These interactions enhance the rigidity and overall thermal stability of the glass network.

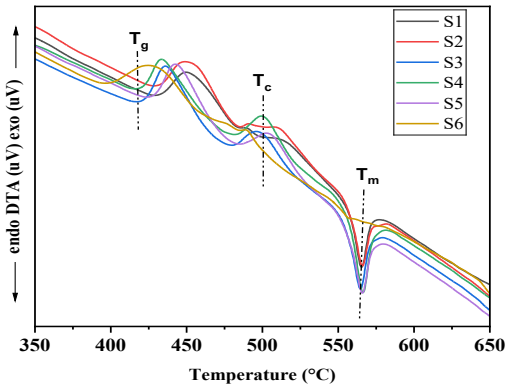

Fig.5. DTA graph of the (40 – *x*) P_2O_5 — 30ZnO — 25Li_2O — 5SrO — (*x*) CH_2COOH glasses

Table 2 DTA characteristics of (40 – *x*) P_2O_5 — 30ZnO — 25Li_2O — 5SrO — (*x*) CH_2COOH glasses with different concentration of CMC.

Sample	Temperature				
	T_g	T_c	T_m	ΔT	H
S1	432	489	564	57	0.770
S2	431	492	566	61	0.824
S3	421	495	564	74	1.072
S4	419	499	566	80	1.194
S5	426	503	566	77	1.222
S6	397	489	556	92	1.373

3.5 *Electrical Analysis*

Impedance spectroscopy, commonly represented as Cole-Cole diagrams or Nyquist plots, is a non-destructive technique used to analyze the electrical properties of inorganic glassy materials, including their behavior under alternating current (AC) conditions across various frequencies and temperatures. This method allows the study of the resistive (Z') and reactive (Z'') components of the impedance, which may appear as semicircles or arcs depending on the material.

As shown in Fig. 6. to Fig.11., Z' and Z'' were measured over a frequency range of 50 Hz to 1 MHz. The bulk resistance (Rb) was determined from the impedance plot as the point where the curve intersects the Z'-axis at low frequencies, and this value was then used to calculate the ionic conductivity of the glass samples.

Table 3 present the CMC molar concentration (%) alongside the corresponding ionic conductivity and activation energy values for the glass system. As shown in Fig 6., sample S3 exhibits the highest ionic conductivity at 0.2 mol% CMC. Beyond this concentration, at 0.3 and 0.4 mol%, the conductivity decreases, followed by a slight increase at 0.5 mol% to 2.53. Fig.6. also indicates that S3 has the lowest activation energy, suggesting that this composition is the most favorable for conductivity, whereas S5 behaves more like an insulator due to its lower conductivity.

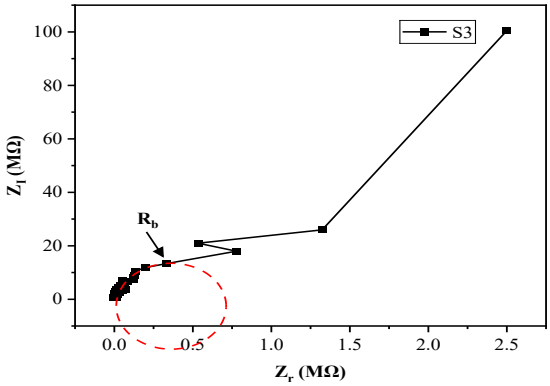

Fig.7. Impedance of sample S3 at room temperature

At low frequencies, the DC conductivity appears as a frequency-independent plateau, while at higher frequencies, the AC conductivity increases with frequency [18]. Fig.7. shows the conductivity of the glass system at different CMC concentrations. The rise in AC conductivity is due to the release of space charges from reduced barrier properties. Conductivity also depends on dopant content and increases with temperature, indicating that electrical conduction in these glasses is thermally activated. Fig.8. shows an activation energy of the glass system with different molar concentration of CMC. Activation energy was calculated using Eq. (6). Glass samples with higher conductivity generally exhibit lower activation energy [12]. The observed variation in activation energy and conductivity may reflect structural changes caused by higher CMC concentrations, which enhance the open structure of non-bridging oxygen ions and facilitate freer movement of charge carriers. The frequency-dependent AC conductivity behavior supports a small polaron hopping mechanism, where the plateau region at low frequencies corresponds to space charge effects and the hopping of charge carriers between available sites [12].

The maximum ionic conductivity (2.89×10^{-7} S·cm^{-1}) and minimum activation energy (1.20×10^{-2} eV) at 0.2 mol% demonstrate that CMC facilitates Li^+ migration by providing polar coordination sites and flexible conduction channels. The conduction mechanism follows the correlated barrier hopping model, where charge carriers jump between localized states assisted by the segmental motion of the surrounding matrix. The carboxylate groups serve as temporary hopping centers, reducing the energy barrier for Li^+ transfer [17]. At higher CMC levels, discontinuity of these paths increases resistance and suppresses conduction. The dielectric constant and loss decrease with frequency due to diminishing dipolar polarization, indicating that interfacial polarization dominates at lower frequencies while electronic and ionic polarization contribute at higher frequencies.

Table 3
The value of molar concentration, conductivity and the activation energy of the glass sample

Molar Concentration of CMC	Conductivity, σ (×10^{-7} Scm^{-1})	Activation energy, E_a (~10^{-2} eV)
0.0	1.77	1.46
0.1	2.49	1.48
0.2	2.89	1.20
0.3	2.78	1.47
0.4	0.44	1.51
0.5	2.53	1.48

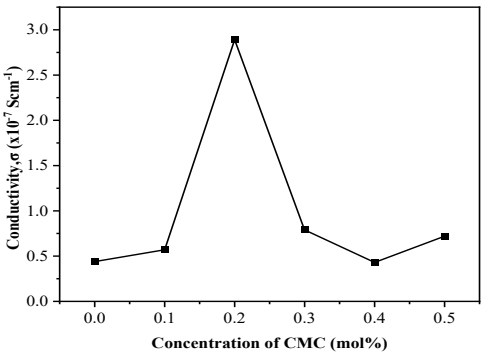

Fig. 7. Conductivity of the glass system with different molar concentration

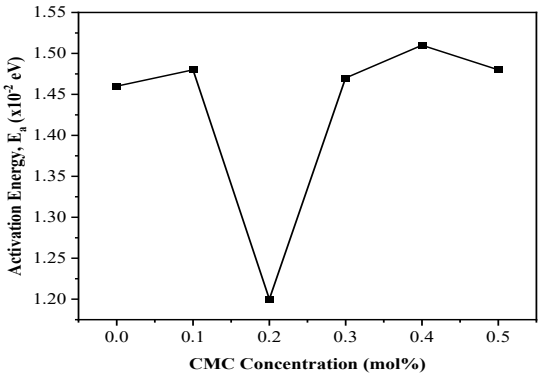

Fig. 8. Activation energy of the glass system with different molar concentration

The relative dielectric constant determines the maximum energy that can be stored in a material, while the dielectric loss factor evaluates the amount of electrical energy absorbed by a dielectric material when subjected to an alternating electromagnetic field [19]. Figure 9. shows the dielectric constant (ε') of sample S3 with frequency. Generally, ε' decreases as frequency increases. This behavior is attributed to dipolar and interfacial polarization, arising from the alignment of permanent dipoles in the direction of the applied electric field and the impedance of mobile charge carriers across interfaces. The dielectric loss (ε'') is influenced by dielectric polarization and DC conduction.

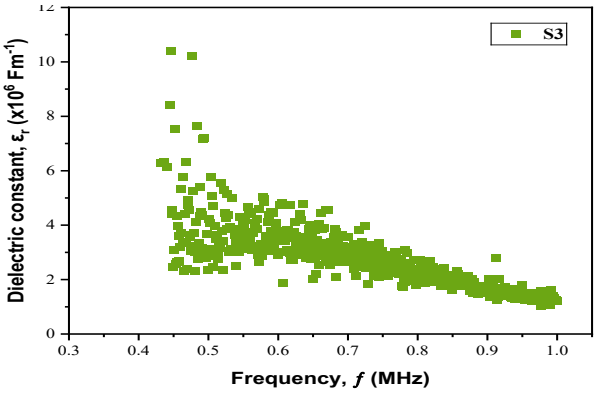

Fig.9. Dielectric constant against frequency of sample S3

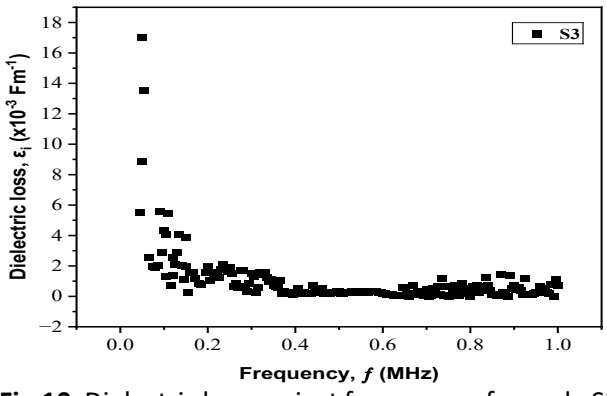

Fig.10. Dielectric loss against frequency of sample S3

At high frequencies, the relatively stable ε' values indicate rapid polarization within the glass samples. Conversely, Fig.10. presents the dielectric loss (ε'') of sample S3 with frequency. Both ε' and ε'' decrease with increasing frequency due to reduced electrical polarization. As frequency rises, the

contribution of charge carriers to polarization diminishes, leading to a continuous decline in ε' and ε'' values [13]. These results suggest that the physical, thermal, and electrical properties of phosphate glasses can potentially be tuned by adjusting the CMC content.

4. Conclusions

Phosphate glasses of composition (40 − x)P_2O_5–30ZnO–25Li_2O–5SrO–(x)CH_2COOH (0.0 ≤ x ≤ 0.5 mol%) were prepared via melt-quenching and characterized for physical, thermal, and electrical properties. All samples were amorphous and transparent. Increasing CMC content enhanced density and packing while reducing molar volume. Thermal analysis showed good stability (T_g: 397–432 °C; T_c: 489–503 °C; T_m: 564–566 °C). The 0.2 mol% CMC glass exhibited the highest ionic conductivity and lowest activation energy, indicating optimal electrical performance. Overall, the 0.2 mol% CMC composition represents the transition point between network compaction and expansion regimes. At low CMC content, hydrogen bonding and metal–carboxylate coordination strengthen the structure, enhance thermal stability, and create efficient Li^+ hopping paths. Beyond this threshold, increased organic disruption introduces excessive free volume, weakens mechanical coherence, and reduces electrical continuity. These results confirm that controlled CMC doping offers a sustainable pathway to fine-tune phosphate glass performance.

Acknowledgement

The authors acknowledge financial support from the Research Management Centre (RMC), Ministry of Higher Education Malaysia (MoHE) under FRGS [R.J130000.7854.5F635 (PY/2023/02164)], the International Grant Nippon Sheet Glass (NSG) [R.J130000.7354.4B743 (PY/2021/02736)], and Dana Universiti Penyelidikan (Caj Analisis Makmal) [Q.J091600.3100.00A37] via UIRL, PPMU, UTM. Appreciation is also extended to colleagues from Universiti Teknologi Malaysia and the Advanced Optical Materials Research Group (AOMRG) for their valuable support and collaboration.

References

[1] Ojovan, Michael I., and William E. Lee. "Immobilisation of radioactive wastes in glass." *An introduction to nuclear waste immobilisation* (2005): 213-249. https://doi.org/10.1016/b978-008044462-8/50019-3

[2] Jerroudi, M., L. Bih, M. Azrour, B. Manoun, I. Saadoune, and Peter Lazor. "Investigation of novel low melting phosphate glasses inside the Na2O–K2O–ZnO–P2O5 system." *Journal of Inorganic and Organometallic Polymers and Materials* 30, no. 2 (2020): 532-542. https://doi.org/10.1007/s10904-019-01213-0

[3] Zaid, M. H. M., K. A. Matori, H. J. Quah, W. F. Lim, H. A. A. Sidek, M. K. Halimah, W. M. M. Yunus, and Z. A. Wahab. "Investigation on structural and optical properties of SLS–ZnO glasses prepared using a conventional melt quenching technique." *Journal of Materials Science: Materials in Electronics* 26, no. 6 (2015): 3722-3729. https://doi.org/10.1007/s10854-015-2891-9

[4] Parchur, A. K., and R. S. Ningthoujam. "Behaviour of electric and magnetic dipole transitions of Eu 3+, 5 D 0→ 7 F 0 and Eu–O charge transfer band in Li+ co-doped YPO 4: Eu 3+." *RSC advances* 2, no. 29 (2012): 10859-10868. https://doi.org/10.1039/c2ra22144f

[5] Higazy, Anwer A., Sanaa El-Rabaie, and Nora Y. Elsheikh. "Structural, Characterization, Optical and Electrical Properties Studies on Li2O–ZnO–P2O5 Glass System." *Menoufia Journal of Electronic Engineering Research* 27, no. 2 (2018): 333-372. https://doi.org/10.21608/mjeer.2018.63266

[6] Rahman, Md Saifur, Md Saif Hasan, Ashis Sutradhar Nitai, Sunghyun Nam, Aneek Krishna Karmakar, Md Shameem Ahsan, Muhammad JA Shiddiky, and Mohammad Boshir Ahmed. "Recent developments of carboxymethyl cellulose." *Polymers* 13, no. 8 (2021): 1345. https://doi.org/10.3390/polym13081345

[7] Siti Norfariza Farhana Mohd Razak, Nur Hazwani Mohd Yusoff, Nurhafizah Hasim, Nur Hidayah Ahmad, Norshahirah Mohamad Saidi, Mohd Fuad Mohamad, and Anis Nazihah Mat Daud. "Structural and Mechanical Properties of Zinc-Strontium-Lithium Phosphate Glass Doped with Carboxymethyl Cellulose." *Semarak International Journal of Material Research* 1, no. 1 (2024): 26-40. https://doi.org/10.37934/sijmr.1.1.2640a

[8] Matori, Khamirul Amin, Mohd Hafiz Mohd Zaid, Hock Jin Quah, Sidek Hj Abdul Aziz, Zaidan Abdul Wahab, and Mohd Sabri Mohd Ghazali. "Studying the effect of ZnO on physical and elastic properties of [(ZnO). sub. x][([P. sub. 2][O. sub. 5]). sub. 1-x] glasses using nondestructive ultrasonic method." *Advances in Materials Science and Engineering* (2015): NA-NA. https://doi.org/10.1155/2015/596361

[9] Nazrin, S. N., M. K. Halimah, F. D. Muhammad, J. S. Yip, L. Hasnimulyati, M. F. Faznny, M. A. Hazlin, and I. Zaitizila. "The effect of erbium oxide in physical and structural properties of zinc tellurite glass system." *Journal of Non-Crystalline Solids* 490 (2018): 35-43. https://doi.org/10.1016/j.jnoncrysol.2018.03.017

[10] Ahmadi, Fahimeh, Rosli Hussin, and Sib Krishna Ghoshal. "Physical and structural properties of dysprosium ion doped phosphate glasses." *Optik* 227 (2021): 166000. https://doi.org/10.1016/j.ijleo.2020.166000

[11] Mohan Babu, M., P. Syam Prasad, S. Hima Bindu, A. Prasad, P. Venkateswara Rao, Nibu Putenpurayil Govindan, N. Veeraiah, and Mutlu Özcan. "Investigations on physico-mechanical and spectral studies of Zn2+ doped P2O5-based bioglass system." *Journal of Composites Science* 4, no. 3 (2020): 129. https://doi.org/10.3390/jcs4030129

[12] Ibrahim, Ali M., A. M. Badr, H. A. Elshaikh, A. G. Mostafa, and Y. H. Elbashar. "Effect of CuO-addition on the dielectric parameters of sodium zinc phosphate glasses."*Silicon* 10, no. 4 (2018): 1265-1274. https://doi.org/10.1007/s12633-017-9599-9

[13] Mohd Abdull Majid, Mohammad Abdull Halim, Nurul Huda Osman, Nizam Tamchek, Nurul Asyikin Ahmad Sukri, Hazeem Ikhwan Mazlan, Nurul Najiha Mazu, Adilah Idris, Josephine Ying Chyi Liew, and Muhammad Mahyiddin Ramli. "Physical, mechanical and electrical properties of chitosan/graphene oxide composite films for copper ions (Cu2+) detection." *Journal of Polymers and the Environment* 31, no. 8 (2023): 3565-3572. https://doi.org/10.1007/s10924-023-02831-z

[14] Li, Chia-Chen, Chi-An Chen, and Meng-Fu Chen. "Gelation mechanism of organic additives with LiFePO4 in the water-based cathode slurries." Ceramics International 43 (2017): S765-S770. https://doi.org/10.1016/j.ceramint.2017.05.315

[15] He, Miaolu, Ze Liu, Lei Wang, Jiani Zhu, Jin Wang, Rui Miao, Yongtao Lv, and Xudong Wang. "Carboxymethylcellulose (CMC)/glutaraldehyde (GA)-modified Ti3C2Tx membrane and its efficient ion sieving performance." Journal of Membrane Science 675 (2023): 121541. https://doi.org/10.1016/j.memsci.2023.121541

[16] Arumughan, Vishnu, Tiina Nypelo, Merima Hasani, and Anette Larsson. "Calcium ion-induced structural changes in carboxymethylcellulose solutions and their effects on adsorption on cellulose surfaces." Biomacromolecules 23, no. 1 (2021): 47-56. https://doi.org/10.1021/acs.biomac.1c00895

[17] Alotaibi, Rajeh, Majed O. Alawad, Khaled D. Khalil, Hana Al-Rafai, Ali H. Bashal, Abdullah A. Alotaibi, and B. Zaidi. "Tailoring the electrical properties of cerium oxide-supported carboxymethyl cellulose composites for electronics and energy storage: insights from density functional theory and molecular dynamics simulations." International Journal of Biological Macromolecules 305 (2025): 141132. https://doi.org/10.1016/j.ijbiomac.2025.141132

[18] Fayad, A. M., M. A. Ouis, R. M. M. Morsi, and R. L. Elwan. "Enhancement of electrical conductivity associated with non-bridged oxygen defects in molybdenum phosphate oxide glass via doping of SrO." Scientific Reports 13, no. 1 (2023): 18321. https://doi.org/10.1038/s41598-023-45333-7

[19] Jlassi, I., N. Sdiri, H. Elhouichet, and M. Ferid. "Raman and impedance spectroscopy methods of P2O5–Li2O–Al2O3 glass system doped with MgO." Journal of Alloys and Compounds 645 (2015): 125-130. https://doi.org/10.1016/j.jallcom.2015.05.025

[20] Melo, B. M. G., M. P. F. Graça, P. R. Prezas, M. A. Valente, A. F. Almeida, F. N. A. Freire, and L. Bih. "Structural and thermal characterization of phosphate based glasses promising for hydrogen absorption." Journal of Non-Crystalline Solids 434 (2016): 28-35. https://doi.org/10.1016/j.jnoncrysol.2015.12.006